A Hybrid Solid-State Beam Scanner for FMCW LiDAR Application

Zhaoyang Zhang,[1] Xufeng Du,[2] Zhiyan Zhou,[1] Qikai Huang,[1] Qiang Zhang,[3] Tingge Dai,[1] Hui Yu,[1] Yuehai Wang,[1] and Jianyi Yang [1,*]

[1] College of Information Science and Electronic Engineering, Zhejiang University, Hangzhou 310027, China
[2] Guofeng Electronics, Manzhouli 021400, China
[3] Zhejiang Lab, Hangzhou 311121, China
Author e-mail address: yangjy@zju.edu.cn

Abstract: We demonstrate a hybrid solid-state beam scanner based on a Si_3N_4 switching array. Two-dimensional beam steering with a 14.3°×9.9° field of view and FMCW ranging operation at a distance of 7.4 m are achieved.

1. Introduction

Due to the huge demand brought by the promotion of autonomous driving and robotics, light detection and ranging (LiDAR) technology has attracted extensive attention in the past decade. To date, various types of on-chip beam scanners have been demonstrated to replace mechanical scanners [1–4]. Optical phased arrays on silicon-on-insulator (SOI) provide an attractive method to perform non-mechanical beam steering [5–7]. However, it still suffers from the extensive and complex active phase shifting, in order to calibrate the stochastic phase errors in the arrayed waveguides [8]. Focal plane switching arrays based on silicon photonics platform and MEMS platform emerge as an alternative approach due to the advantages of compact size, low power consumption and simple control [9,10]. Among them, beam scanners based on Mach–Zehnder interferometer (MZI) abandon the mechanical moving parts entirely. In addition, ultra high-speed and low-loss optical switches can be obtained by integrating novel materials with high Pockels coefficients [11,12]. In this work, we demonstrate a hybrid solid-state beam scanner based on a Si_3N_4 switching array and a blazed grating. The output beam is steered across the 14.3° × 9.9° field of view (FOV) with beam divergence less than 0.1°. In addition, a ranging distance of 7.4 m is achieved by combining the proposed beam scanner and the frequency-modulated continuous-wave (FMCW) technology.

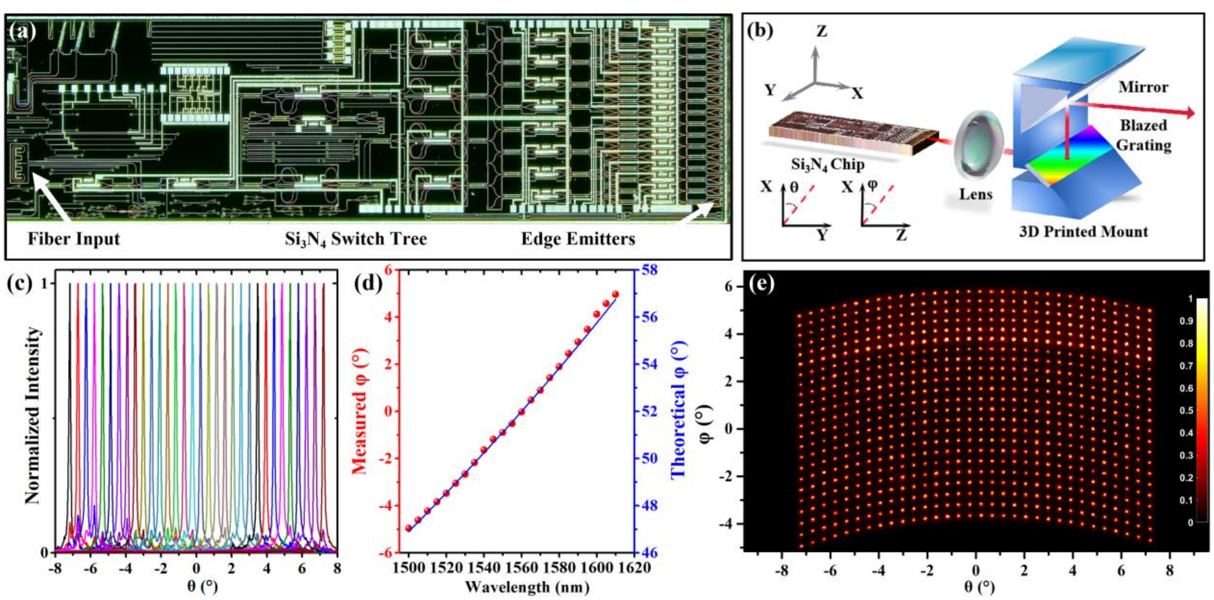

Fig. 1. (a) Microscope photograph of the fabricated Si_3N_4 switching array chip. (b) Schematic of the hybrid solid-state beam scanner. (c) Intensity cuts in θ-direction of 32 separate beams at different angles. (d) Measured beam scanning result and the theoretical value of the transmission grating in φ-direction versus the working wavelength. (e) Two-dimensional beam scanning observed on the screen.

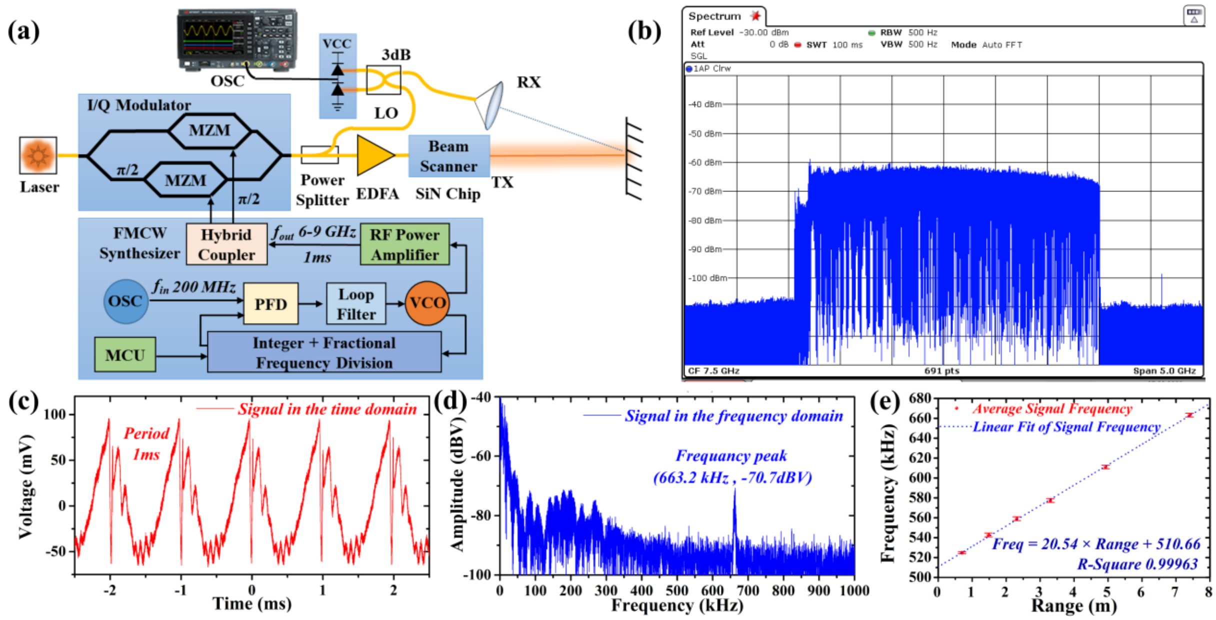

Fig. 2. (a) Experimental setup of the FMCW ranging operation using the beam scanner. (b) The spectrum of the PLL based FMCW synthesizer. (c) and (d) are the time domain and frequency domain signals corresponding to the target of 7.4 m, respectively. (e) Measured beat frequency versus the ranging distance.

2. Device Fabrication and Beam Steering

An optical micrograph of the 32-channel Si_3N_4 switching array with an overall footprint of 2.2 mm × 10 mm is shown in Fig. 1 (a). The device is fabricated on an 8-inch wafer with a 400 nm-thick PECVD Si_3N_4 layer by Advanced Micro Foundry. Light is coupled into the chip from a grating coupler. Next, a five-layer binary tree formed by cascaded Si_3N_4 MZI switches routes the incident beam to 32 channels. Thermo-optics phase shifters are used to control the on-chip light path. The edge emitters are etched facet inverse tapers with a tip width of 300 nm. The pitch between two adjacent edge emitters is 65 µm. The schematic of the solid-state beam scanner is depicted in Fig. 1 (b). Beam emitted from the chip is collimated by an aspherical lens (f = 8.0 mm, NA = 0.5). Then the output beam is aligned to a lithographically patterned diffraction transmission grating (966.18 lines/mm) at the Littrow angle. Next, a 45° aluminum-coated mirror fixed in the 3D printed mount is used to deflect the beam direction. To characterize the beam steering, we set a screen in front of the beam scanner at a distance of 2.1 m. An infrared camera records the beam profile on the screen. As shown in Fig. 1 (c), the main beam is steered across a range of 14.3° in θ-direction by toggling the optical switches. Though phase errors still exist in the Si_3N_4 photonic integrated circuit, the initial phase calibration takes only a few minutes. This problem can be further solved by the real-time feedback control with on-chip power monitors. The angular step between two adjacent points is 0.46°, which can be much decreased by enlarging the array size in our future work. A beam steering range of 9.9° in the φ-direction is achieved by tuning the wavelength from 1500 nm to 1610 nm, as shown in Fig. 1 (d). The steering efficiency thus is around 0.09°/ nm, which is higher than the on-chip Si_3N_4 grating antenna in [13]. The demand of wideband tunable laser with narrow linewidth still hinders further cost reduction. However, it can be solved by using the massive coherent laser based on the microcomb in [14]. Finally, two-dimensional beam steering is achieved by wavelength tuning and switching of channels, as shown in Fig 1. (e). The beam divergency in both directions is measured to be < 0.1°.

3. FMCW Ranging Operation

The setup for FMCW ranging operation is shown in Fig. 2 (a). The FMCW RF signal is provided by the frequency synthesizer based on a fractional-N phased-locked loop (PLL). It generates sawtooth chirps with a period of 1 ms. The chirp range is approximately from 6 GHz to 9 GHz, as shown in Fig. 2 (b). Then the chirped laser light is generated by using an optical single sideband modulator. A 3dB optical power splitter distributes the output of the modulator into two components: one goes straight to the balance detector as the local reference light, and the remaining is amplified by an Erbium-doped fiber amplifier (EDFA) as the input of the Si_3N_4 chip. The backscattered light from the target is collected by a fiber collimator and routed to the balanced detector. An oscillograph records the output of the balanced photodetector and performs real-time FFT analysis. Representative beat signals in the time domain and the frequency domain of a target at 7.4m away are depicted in Fig. 2 (c) and Fig. 2 (d), respectively. Figure 2 (e) shows the measured beat frequency when the target distance varies from 0.7 m to 7.4 m. A strong linear correlation between the beat frequency and the target distance is observed. The slope of the linear fit is around 20.54 kHz/m, which is in line with the chirp slope of $\sim$ 3 MHz/μs. It is worth noting that the intercept at the frequency axis comes from the fixed fiber length difference. The chirp slope can be further increased by using FMCW PLL ICs [15], in order to speed up the ranging operation.

4. Conclusion

In conclusion, we demonstrate a hybrid solid-state beam scanner based on the Si_3N_4 switching array. The combination of the edge emitter and the external transmission grating improves the beam quality as well as the optical emission efficiency. Besides, no prism lens with special designs and mechanical moving components exist in the easily implemented beam scanner. Two-dimensional beam steering with a FOV of 14.3° × 9.9° is achieved by switch toggling and wavelength tuning. Furthermore, FMCW ranging operation up to 7.4 m is also presented by using the Si_3N_4 switching array as the transmitter. Our measurements indicate that the proposed hybrid solid-state beam scanner is a scalable and flexible solution for the next-generation FMCW LiDAR.

5. References

[1] D. N. Hutchison, J. Sun, J. K. Doylend, R. Kumar, J. Heck, W. Kim, C. T. Phare, A. Feshali, and H. Rong, “High-resolution aliasing-free optical beam steering”, Optica **3**, 887–890 (2016).

[2] H. Ito, Y. Kusunoki, J. Maeda, D. Akiyama, N. Kodama, H. Abe, R. Tetsuya, and T. Baba, “Wide beam steering by slow-light waveguide gratings and a prism lens”, Optica **7**, 47–52 (2020).

[3] J. Park, B. G. Jeong, S. I. Kim, D. Lee, J. Kim, C. Shin, C. B. Lee, T. Otsuka, J. Kyoung, S. Kim, K.-Y. Yang, Y.-Y. Park, J. Lee, I. Hwang, J. Jang, S. H. Song, M. L. Brongersma, K. Ha, S.-W. Hwang, H. Choo, and B. L. Choi, “All-solid-state spatial light modulator with independent phase and amplitude control for three-dimensional LiDAR applications”, Nat. Nanotechnol. **16**, 69–76 (2021).

[4] R. Li, S. Hu, X. Gu, and F. Koyama, “Solid-state slow-light beam scanner with ultra-large field of view and high resolution”, J. Light. Technol. **40**, 1855–1861 (2022).

[5] C. V. Poulton, M. J. Byrd, P. Russo, E. Timurdogan, M. Khandaker, D. Vermeulen, and M. R. Watts, “Long-range LiDAR and free-space data communication with high-performance optical phased arrays”, IEEE J. Sel. Top. Quantum Electron. **25**, 1–8 (2019).

[6] Y. Li, B. Chen, Q. Na, Q. Xie, M. Tao, L. Zhang, Z. Zhi, Y. Li, X. Liu, X. Luo, G. Lo, F. Gao, X. Li, and J. Song, “Wide-steering-angle high-resolution optical phased array”, Photon. Res. **9**, 2511–2518 (2021).

[7] W. Xu, Y. Guo, X. Li, C. Liu, L. Lu, J. Chen, and L. Zhou, “Fully integrated solid-state lidar transmitter on a multi-layer silicon-nitride-on-silicon photonic platform”, J. Light. Technol. pp. 1–10 (2022).

[8] T. Komljenovic and P. Pintus, “On-chip calibration and control of optical phased arrays”, Opt. Express **26**, 3199–3210 (2018).

[9] X. Zhang, K. Kwon, J. Henriksson, J. Luo, and M. C. Wu, “A large-scale microelectromechanical-systems-based silicon photonics LiDAR”, Nature **603**, 253–258 (2022).

[10] C. Rogers, A. Y. Piggott, D. J. Thomson, R. F. Wiser, I. E. Opris, S. A. Fortune, A. J. Compston, A. Gondarenko, F. Meng, X. Chen, G. T. Reed, and R. Nicolaescu, “A universal 3D imaging sensor on a silicon photonics platform”, Nature **590**, 256–261 (2021).

[11] F. Eltes, C. Mai, D. Caimi, M. Kroh, Y. Popoff, G. Winzer, D. Petousi, S. Lischke, J. E. Ortmann, L. Czornomaz, L. Zimmermann, J. Fom-peyrine, and S. Abel, “A BaTiO3-based electro-optic Pockels modulator monolithically integrated on an advanced silicon photonics platform”, J. Light. Technol. **37**, 1456–1462 (2019).

[12] K. Alexander, J. P. George, J. Verbist, K. Neyts, B. Kuyken, D. Van Thourhout, and J. Beeckman, “Nanophotonic Pockels modulators on a silicon nitride platform”, Nat. Commun. **9**, 3444 (2018).

[13] C. Li, X. Cao, K. Wu, G. Qiu, M. Cai, G. Zhang, X. Li, and J. Chen, “Blind zone-suppressed hybrid beam steering for solid-state LiDAR”, Photon. Res. **9**, 1871–1880 (2021).

[14] J. Riemensberger, A. Lukashchuk, M. Karpov, W. Weng, E. Lucas, J. Liu, and T. J. Kippenberg, “Massively parallel coherent laser ranging using a soliton microcomb”, Nature **581**, 164–170 (2020).

[15] H. Shanan, D. Dalton, V. Chillara, and P. Dato, “A 9-to-12GHz coupled-RTWO FMCW ADPLL with 97fs rms jitter, -120dBc/Hz PN at 1MHz offset, and with retrace time of 12.5 ns and 2 μs chirp settling time”, in 2022 IEEE International Solid- State Circuits Conference (ISSCC), vol. 65 (2022), pp. 146–148.